

AN EFFECTIVE INDEX FOR ISLANDING DETECTION BASED ON FAST DISCRETE S-TTRANSFORM

Solgun SALIMI¹, Amangaldi KOOCHAKI¹, Amin HAJIZADEH²

¹Electrical Engineering Department, Aliabad Katoul Branch, Islamic Azad University,
Daneshgah Blvd, Aliabad Katoul, Iran

²Department of Energy Technology, Faculty of Engineering and Science, Aalborg University,
Niels Bohrsvvej 8, 6700 Esbjerg, Denmark

solgun.salimi@gmail.com, koochaki@aliabadiu.ac.ir, aha@et.aau.dk

DOI: 10.15598/aece.v17i2.3340

Abstract. *Passive methods of islanding detection have the advantage of not perturbing the system, but they suffer from large Non-Detection Zone (NDZ) and unpredictable detection time. In this paper, a new passive scheme for islanding detection, based on estimating a new index derived from summation of impedance values in all frequencies along the time at the Point of Common Coupling (PCC), is introduced using Fast Discrete S-Transform (FDST) method. The proposed method maintains both time and frequency information and as a result, helps to decrease the detection time. A frequency dependent model is proposed for characterizing the interconnection changes when islanding happens. The Cumulative Impedance Index (CII) is proposed to discriminate between islanding condition and normal operation. This technique is combined with under/over voltage protection method to decrease NDZ. Simulations for different conditions of normal and islanding operations verify the proposed algorithm. In all cases, islanding is detected within 0.01 s, and NDZ is decreased to 1 % of power mismatch between local load and Distributed Generator (DG) output. The results demonstrate the capability of the method to islanding detection with minimum delay and least NDZ.*

Keywords

Discrete S-Transform, impedance deviation, Non-detection zone, passive islanding detection.

1. Introduction

Penetration of DGs in Electrical Power System (EPS) brings great challenges such as islanding detection and prevention [1], [2], [3], [4] and [5]. Islanding is a case in which the DG continues energizing a part of the distribution system which is disconnected from the grid. Islanding can cause negative effects on the network and DG, like safety hazards to personnel, equipment and EPS, as well as power quality problems, even though the main is restored immediately [6]. According to IEEE Std. 1547-2003, maximum acceptable delay for detection of islanding condition is 2 s [3] and [4]. In addition, according to IEEE 929-1988 standard, if islanding occurs, DG should be interrupted [3] and [4]. Therefore, the development of islanding detection procedures is one of the main topics of literature.

In passive methods, some parameters including voltage, frequency, or current at PCC are measured to detect occurrence of islanding using Under/Over Voltage Protection (UVP/OVP) [7], Under/Over Frequency Protection (UFP/OFP) [7], and Vector Shift (VS) [8]. More methods that are sensitive have been introduced to improve passive techniques, consisting of the phase jump [9], frequency deviation rate [10], output power change rate [11], calculation of total harmonic distortion [12], power spectral density [13] and harmonic impedance of grid [14]. These methods, although they are simple in operation, have a larger NDZ when the generation and load in an islanded section are nearly equal [14]. Compared to passive approaches, response time of active methods is shorter and their NDZ is smaller. However, the power quality of the EPS will be decreased due to the perturbation [8]. Advanced filtering methods and spectral decomposition have also been developed, including the pattern recognition of transient signals [15], wavelet singular entropy [16],

and intelligent systems [17]. These methods are based on feature extraction, classifications and data training process thus these are dependent on the structure of network and time-consuming.

Recently, numerous methods for estimation of grid impedance have been developed to improve islanding detection in EPSs with power converters [18], [19], [20] and [21]. Passive methods exploit the measurement of harmonic voltage and current which exist in the system, inherently, to calculate the impedance. Time-frequency analysis algorithms such as FFT and wavelet transform have been used to do this estimation, but time information gets lost in FFT [14] and [22]. The S-Transform (ST) is a powerful technique which retains both time and frequency information, so it is very useful in signal processing and extracting the features [23] and [24]. The ST maintains the absolute phase information by using the Fourier transformation kernel. A frequency-dependent window function is applied at high frequencies and produces high time and frequency resolution; so, this method is not dependent on certain frequencies and will not lose its effectiveness in absence of them [25]. FDST reduced complexity of calculations using an intelligent frequency selection technique and removing unnecessary data [26].

This paper presents a new algorithm to detect islanding based on FDST, which is not restricted by selecting some harmonics. In this method, a new feature is proposed to distinguish islanding condition from normal operation. The feature is extracted using FDST of current and voltage measured at PCC and it is based on changes of cumulative impedance of all frequencies. This feature could be used for threshold selection with large setting margins. Combining this new method with UVP/OVP method has made the approach more reliable. The DGs may consist of power converters or not. The proposed method has been assessed in several cases consisting of connecting and disconnecting huge loads and Non-linear loads to the grid, motor starting and presence of noise. In all studied cases, new method has operated properly, having considerable margin of threshold and small NDZ.

The paper is organized as follows; Sec. 2. presents the model based on impedance interconnection and describes the FDST algorithm. In Sec. 3. an algorithm for islanding detection is proposed based on FDST and feature extraction. The proposed method is verified with the simulation data in Sec. 4. In Sec. 5. threshold setting and NDZ of new method are explained. Finally, conclusions are presented in Sec. 6.

2. System Modelling and Backgrounds

2.1. Circuit Model

Figure 1 shows interconnection between the DG and the EPS, consisting of a local load, Z_L , connected at the PCC to the DG and network via a breaker, B, and the grid impedance, Z_g .

Non-linear loads which usually exist in the network are sources of harmonic current. Inverter-based DGs produce harmonics at the result of Pulse Width Modulation (PWM) strategy of converters. Also, DGs without inverters may have inherent harmonics. An ideal current source can be used for modelling the non-linear loads, in order to facilitate the analyzing of these systems [15] and [16]. So, the network is displayed as an ideal current source. A current source is used to model the DG as well. When the breaker, B, suddenly opens, islanding phenomenon occurs. Thus, a quick change occurs in the system topology, which can be determined by changes in the impedance [14].

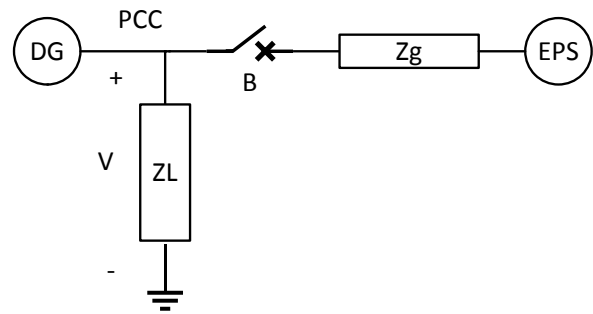


Fig. 1: DG interconnection topology.

In normal condition, the breaker, B, is closed, and the DG sees parallel impedance of Z_L and Z_g . By opening the breaker, islanding condition is occurred and impedance is seen by DG changes to Z_L . Therefore, the harmonic components of current and voltage at PCC change suddenly.

Theoretically, impedance which is seen by DG in normal operation is calculated as follow:

$$Z_{pcc}^n = \frac{Z_l Z_g}{Z_l + Z_g}. \quad (1)$$

And in islanding operation:

$$Z_{pcc}^i = Z_l. \quad (2)$$

By considering a parallel RLC load as the local load $\left(Z_l(s) = \frac{sLR}{s^2LCR + sL + R}\right)$ and a series RL load as the grid impedance $(Z_g(s) = R_g + sL_g)$:

$$Z_{pcc}^n = \frac{RL L_g s^2 + RR_g L s}{RL L_g C s^3 + (RL L_g + LL_g + RR_g LC) s^2 + R_g L s + RR_g}. \quad (3)$$

$$Z_{pcc}^i = \frac{sLR}{s^2LCR + sL + R}. \quad (4)$$

Practically, the frequency dependent impedance that can be seen by the DG at PCC can be calculated using FDST of voltage and current at PCC.

2.2. Discrete S-Transform

The S-transform is a new time–frequency analysis technique, which is derived from both the STFT and the Continuous Wavelet Transform (CWT) [24]. Discrete Fourier transform (DFT) of $X_{i(i=1,2,\dots,N)}$, with N sample is defined by

$$Y = \text{DFT}(X_i) = [y_1 \quad \dots \quad y_n \quad \dots \quad y_N], \quad (5)$$

where

$$y_n = \sum_{i=1}^N X_i \exp\left(\frac{-2\pi j(n-1)(i-1)}{N}\right), i = \sqrt{-1}. \quad (6)$$

The matrix \mathbf{H} is obtained from rotating and concatenating of Y :

$$\mathbf{H}_{M \times N} = \begin{bmatrix} y_2 & y_3 & \dots & y_N & y_1 \\ y_3 & y_4 & \dots & y_1 & y_2 \\ \dots & \dots & \dots & \dots & \dots \\ y_M & y_{M+1} & \dots & y_{M-2} & y_{M-1} \\ y_{M+1} & y_{M+2} & \dots & y_{M-1} & y_M \end{bmatrix}, \quad (7)$$

where according to Nyquist sampling theorem, M is equal to half of N . By considering the N as a positive even integer value, time–frequency transforms are applied on M discrete frequencies.

A two-dimensional Gaussian window, $W_{M \times N}$, is formed to localize time and frequency domain. Each element of this window is as below:

$$W_{(m,n)} = \exp\left(\frac{-2\pi^2(n-1)^2 F}{(a + bm^c)^2}\right) + \exp\left(\frac{-2\pi^2(N-n+1)^2 F}{(a + bm^c)^2}\right), \quad (8)$$

where $m = 0, 1, \dots, M, n = 0, 1, \dots, N$ and F is a window factor. Multiplying \mathbf{H} with W results frequency-domain information:

$$G_{(m,n)} = \mathbf{H}_{(m,n)} \times W_{(m,n)}. \quad (9)$$

The S-Transform matrix is obtained by taking Inverse Discrete Fourier Transform (IDFT) as below:

$$\mathbf{S}_{M \times N} = \begin{bmatrix} s(f_1, t_1) & \dots & s(f_1, t_n) & \dots & s(f_1, t_N) \\ \dots & \dots & \dots & \dots & \dots \\ s(f_m, t_1) & \dots & s(f_m, t_n) & \dots & s(f_m, t_N) \\ \dots & \dots & \dots & \dots & \dots \\ s(f_M, t_1) & \dots & s(f_M, t_n) & \dots & s(f_M, t_N) \end{bmatrix}. \quad (10)$$

Each element of this matrix is defined as below:

$$s_{(m,n)} = \left(\frac{2}{N}\right) \sum_{i=1}^N G_{(m,i)} \exp\left(\frac{-2\pi j(n-1)(i-1)}{n}\right). \quad (11)$$

The ST of $X(t)$ can parse the signal into a complex time–frequency matrix. The matrix contains vectors of frequency at a certain time at rows, and vectors of time at a certain frequency at columns. Also, it contains much information consisting of amplitude, phase, and frequency. In this paper, by using FDST, the time–frequency information of impedance signal was represented by an amplitude matrix [27].

3. Proposed S-Transform Based Islanding Detection

The main idea of this paper is to detect islanding condition with the least NDZ. The FDST is employed to feature extraction from the measured voltage and current of PCC. The proposed method includes detection of perturbation and steps for discriminating the islanding condition. The method introduced a cumulative impedance index for Islanding detection.

3.1. Perturbation Detection Step

The UVP/OVP and UFP/OFP schemes are the most common solutions for islanding detection exploiting changes in the frequency and voltage which stem from mismatches of active and reactive power [28] and [29]. These methods must be included in all grid-connected inverters, not only as a protection to keep the equipment safe but also as an islanding detection scheme.

At the instant, before islanding, if $\Delta P > 0$, the domain of U_{pcc} changes, and the UVP/OVP could identify the variation and prevent islanding. If $\Delta Q > 0$, there is a shift in phase of load voltage, therefore inverter changes frequency of output current and frequency of U_{pcc} consequently, so UFP/OFP could distinguish this change.

If $\Delta P = \Delta Q = 0$, means output power of DG matches to the required power at load, the changes in amplitude or frequency of U_{pcc} will be insufficient to ac-

tivate standard protection devices. Also to prevent nuisance trips, some threshold for voltage and frequency should be considered. Therefore, this method has relatively large NDZ, which makes it fail under certain conditions.

For improving the performance of detection, more sensitive procedure has been introduced. By any disturbance in voltage or frequency, the process is started and at first, the UVP/OVP or UFP/OFP method is activated to check if this disturbance is beyond the threshold values. If it is so, trip signal is activated directly. Otherwise, next steps will check.

3.2. Islanding Discrimination Algorithm

As expressed in Subsec. 2.1. the frequency dependent impedance changes when islanding occurs. The feature is constructed based on impedance frequency spectrum which has obtained from S-matrix of a half cycle of voltage and current signals. Figure 2 and Fig. 3 present the frequency spectrum of impedance which is seen for the typical network in normal and islanding conditions from PCC. It can be seen that there is a clear difference in area between the fundamental frequency (50 Hz) up to 15th harmonic (750 Hz) of impedance ("A") in two conditions (before and after islanding). In Fig. 4, one branch of a grid, consisting noticeable loads, is disconnected without leading to islanding, and as can be seen from the figure, the change in ("A") is very small, compared to islanding situation. Amplitude of each frequency component of impedance is calculated using summation of rows in the S-matrix. The mathematical formulation of the feature is performed using trapezoidal method:

$$ZI_i = \frac{h_{15} - h_1}{2N} \sum_{k=1}^N (Z(h_{k+1}) + Z(h_k)), \quad (12)$$

$$CII_i = |ZI_i - ZI_{i-1}|, \quad (13)$$

where $N, h_i, Z(h_i)$ are the number of equally spaced panels, harmonic order and its amplitude, respectively. Differences between two consecutive ZI_i s are calculated and named as CII .

Simulations show that when islanding happens there is a considerable difference between ZI s before and after islanding, therefore there is a peak in CII values and this is the new index for islanding detection introduced in this paper. The flowchart of the proposed method is illustrated in Fig. 5.

The process starts by any change, which occurred, in measured voltage at PCC. If this value is over the assumed threshold value, $88\% < U < 110\%$ [30], it means that islanding has occurred. But if it is between these values it must be checked if this change

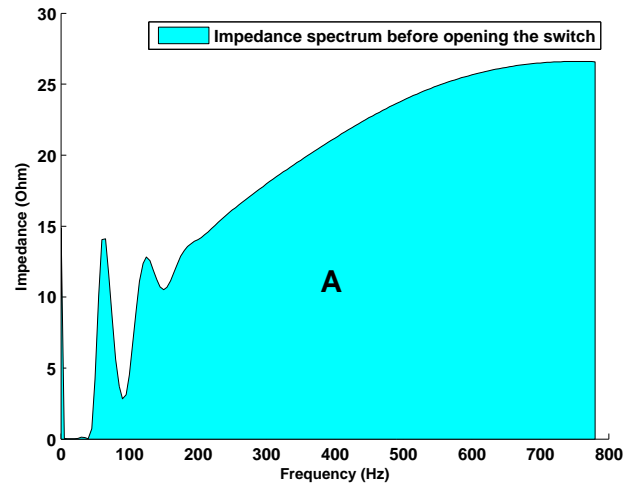


Fig. 2: Impedance spectrum in normal condition.

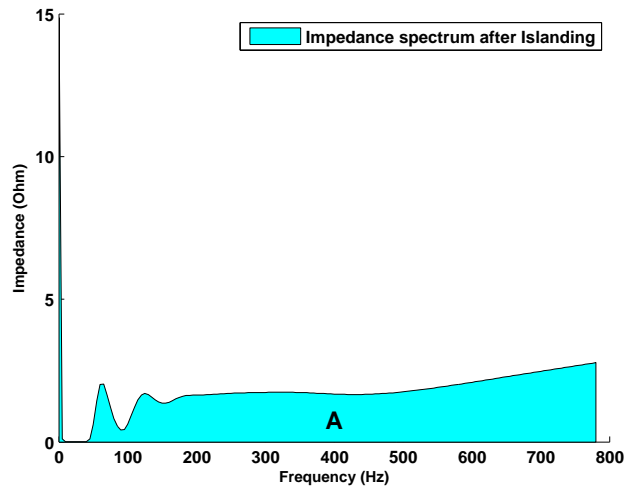


Fig. 3: Impedance spectrum after islanding.

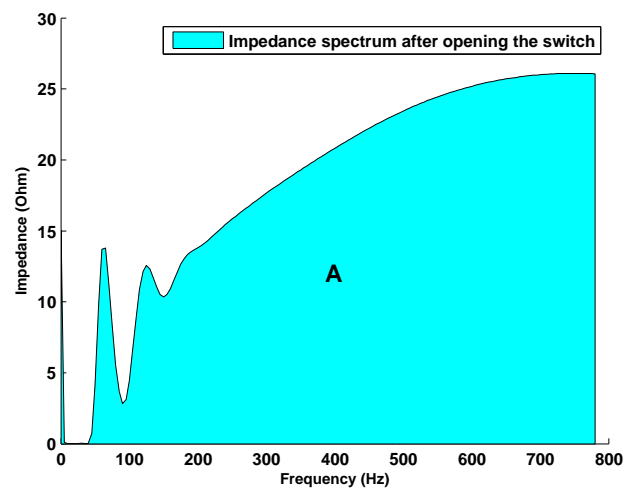


Fig. 4: Impedance spectrum after branch disconnecting.

happened as a result of worst condition islanding or as a result of noise. So, FDST of voltage and current

are computed. The frequency dependent impedance is computed by dividing the U_{pcc} magnitude to I_{pcc} magnitude at corresponding frequencies. ZI is computed for specified time intervals as explained above. Then, CII is calculated and checked. If change of CII is over the threshold value, a trip signal is activated and the DG is disconnected from the EPS, consequently.

Selecting smaller time interval could result in faster detection of islanding, but it also should be large enough to avoid getting affected by noise or any other sorts of destructions.

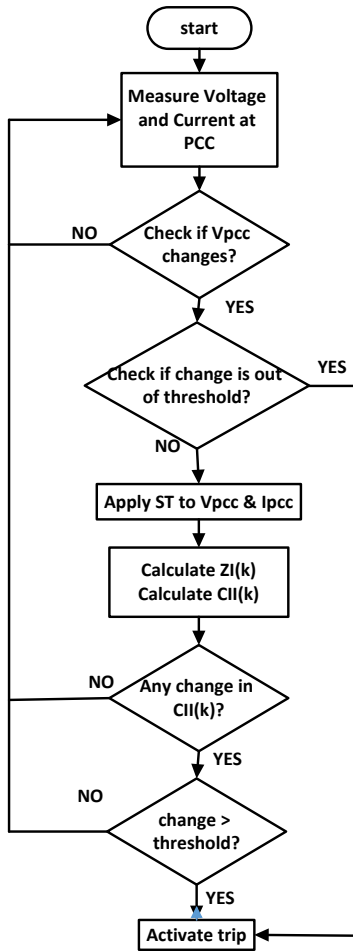


Fig. 5: Flowchart of the proposed method.

4. Simulation Results

To verify the proposed method, it has been implemented in MATLAB and a practical distribution network is simulated in EMTDC/PSCAD (Fig. 6). The transmission substation is 10/0.4 kV, which is feeding a commercial area. The power factor of loads is 0.85; for each load the maximum demand in kVA is written in Fig. 6. A 3 kW inverter-based DG is connected to the network. Parameters of RLC local load are as

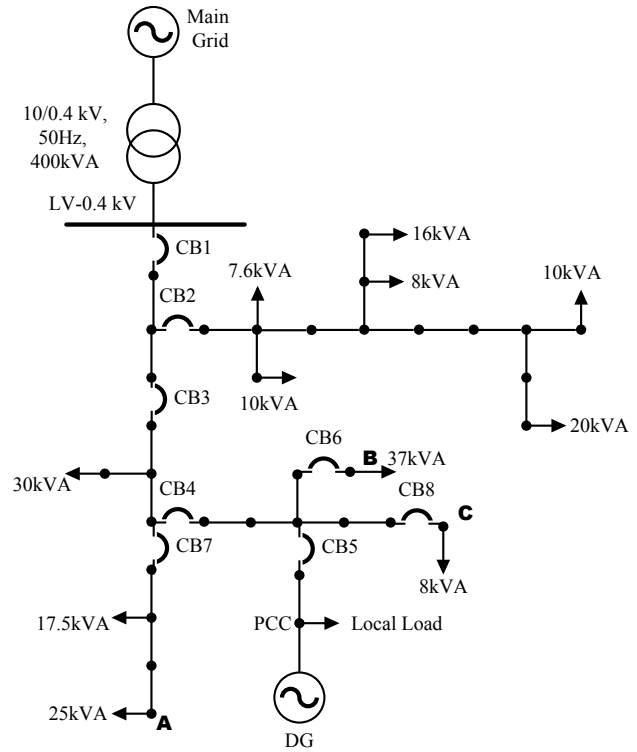


Fig. 6: A practical LV distribution network.

$R = 16.13 \Omega$, $L = 20.5 \text{ mH}$, $C = 493.25 \mu\text{F}$. These parameters put the DG in situation of power balance. To verify the method, 200 simulations in the form of five cases are studied. In Case 1, normal operation is considered. In this case, configuration of the system changes at 0.6 s, by opening the breaker B2. Case 2 and Case 3 study islanding conditions, which occur as a result of opening breakers B4 and B5, respectively. In Case 2, a large power imbalance is created between load and generation, while in Case 3, power is balanced approximately. In Case 4 and Case 5, an inductive and a non-linear load are connected to the network at 0.4 s respectively.

Case 1: Figure 7 and Fig. 8 show the results of simulations for Case 1. In this case, one of the branches is disconnected from network by opening the breaker B2 which leads to change in the grid impedance. As can be seen from Fig. 8, the amount of change in ZI is ignorable and CII is small (just less than one unit). Thus, by selecting reasonable threshold, it doesn't produce a trip.

Case 2: Fig. 9 and Fig. 10 display the simulation results of Case 2. In this case, islanding occurs when breaker B4 opens at 0.6 s and disconnects a large amount of load from the network, so that a considerable fall emerges at ZI , with a considerable rise (about 17 units) in CII . Thus, islanding is detected within

0.01 s. Figure 10 indicates that in such cases with a large power imbalance, islanding condition can be easily identified by monitoring the voltage at PCC. Same results have been achieved by opening the CB7.

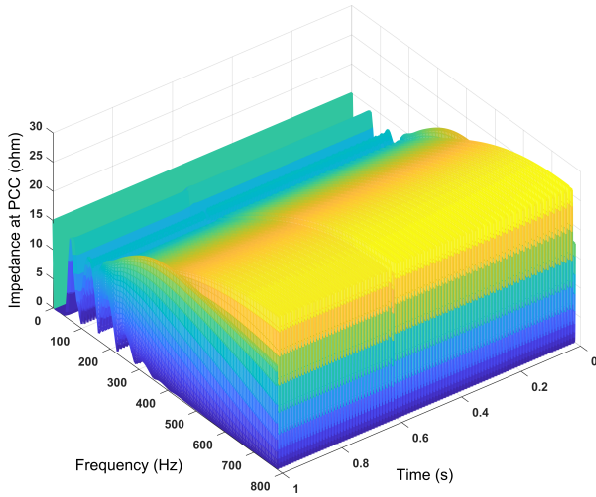


Fig. 7: Calculated impedance at PCC for Case 1.

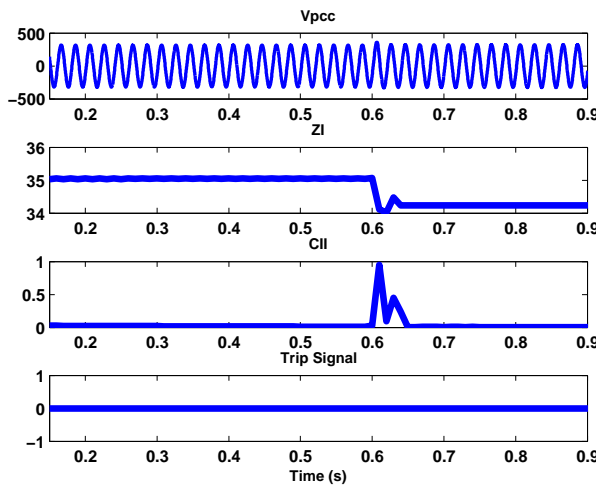


Fig. 8: System response for Case 1.

Case 3: In Case 3, power between DG and local load is in balance, approximately. This is the worst case to detect islanding, in which UVP/OVP and UFP/OFM methods cannot detect it. As Fig. 11 and Fig. 12 illustrate, change of ZI and magnitude of CII is remarkable (about 14 units). Thus, the new proposed method easily detects the occurrence of islanding immediately. As can be seen from Fig. 12, there is not any visible change in V_{pcc} , but according to the proposed method and Fig. 12, there is a considerable change in CII . Therefore, islanding is detected.

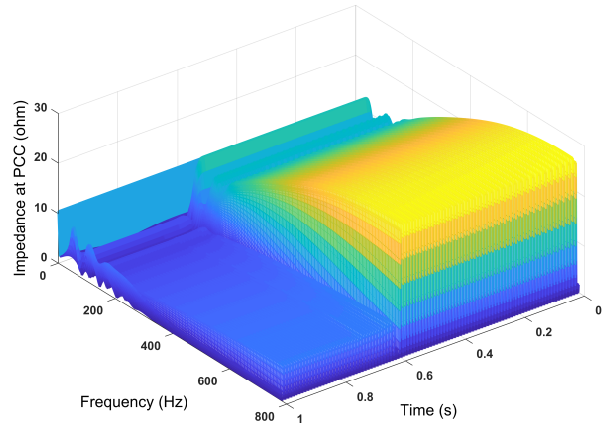


Fig. 9: Calculated impedance at PCC for Case 2.

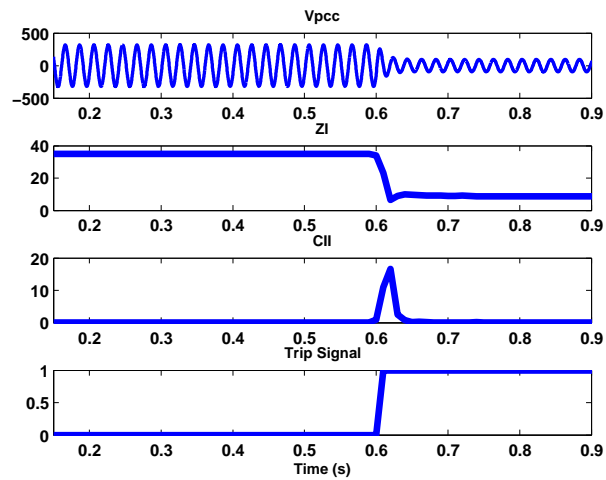


Fig. 10: System response for Case 2.

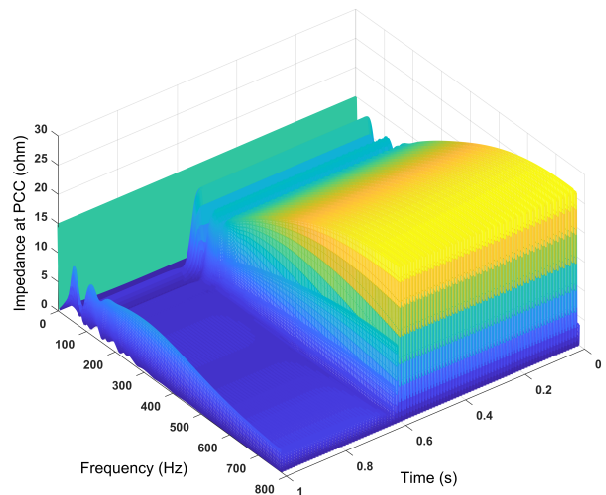


Fig. 11: Calculated impedance at PCC for Case 3.

Case 4: In this case, a 37 kVA motor is added to the grid at point B to study the effects of connecting and disconnecting of inductive loads on the proposed method. Comparing to other loads of the sim-

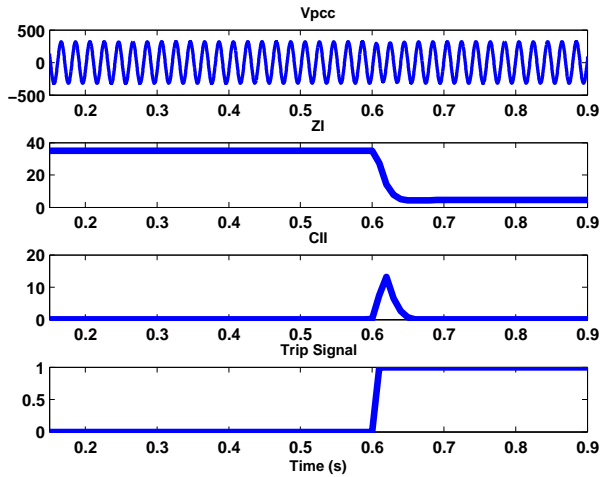


Fig. 12: System response for Case 3.

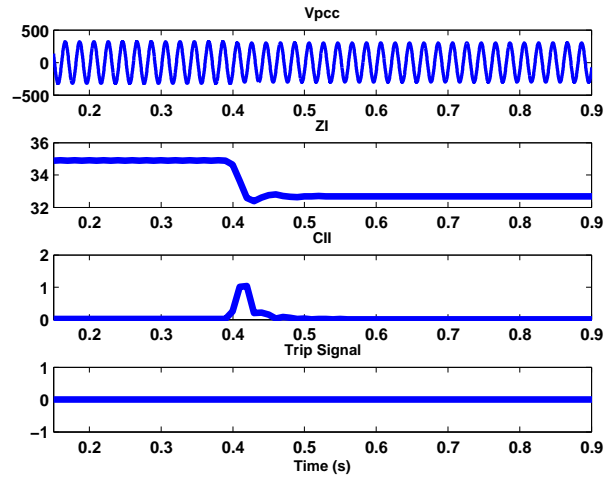


Fig. 14: System response for Case 4.

ulated network, the size of motor is significant. Thus, the network’s parameters are affected. Figure 13 and Fig. 14 show the results of this study. Motor is added at 0.4 s and as it is obvious in Fig. 14, *CII* is not big enough (less than 1 unit) to activate a trip signal.

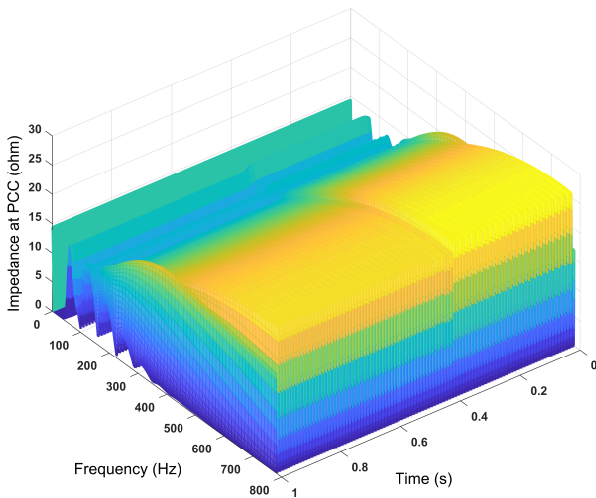


Fig. 13: Calculated impedance at PCC for Case 4.

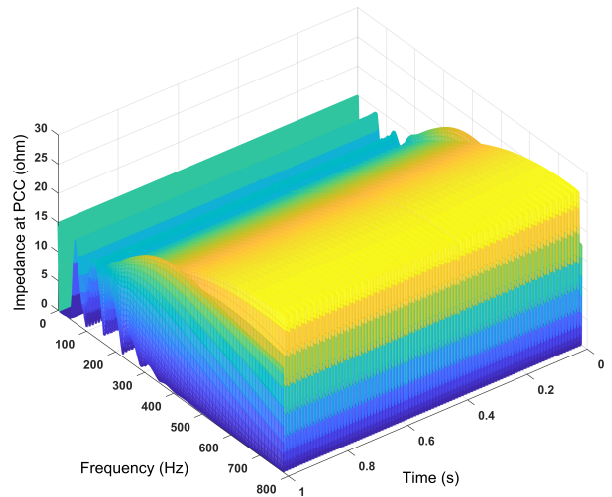


Fig. 15: Calculated impedance at PCC for Case 5.

Case 5: Non-linear loads are the most problematic loads in grids due to their harmonics and they can affect protective equipment and solutions. In this case, a non-linear load consisting of a three-phase diode is added to the grid at point C, at 0.4 s. Results are illustrated in Fig. 15 and Fig. 16. In this case, although there is a variation in the proposed index as a result of the Non-linear load, *CII* is small. The only considerable change happens at the moment of connecting this load to the network (less than 0.4 unit) which is still less than considered threshold to activate a trip signal.

In order to study the effect of noise on the proposed method, white noise with *SNR* = 20 dB is added to the measured voltage. All simulations are repeated with this noise. Simulation results show that the proposed method is not sensitive to noise. In all cases, the detecting time is dependent on the selected time interval of algorithm. Detection time is around 0.01 s, which in comparison with other passive methods, Less than 20 ms - Within 2 s.

5. Threshold Setting and NDZ

For setting the threshold value correctly, the worst islanding situation should be considered and a calculated *CII* should be adjusted as threshold value. On the other hand, in order to avoid nuisance trips, this value cannot be smaller than *CII* of normal operations (i.e. load switching). In this paper, *CII* in the worst case of

Tab. 1: Comparison of some of islanding detection methods with the proposed method.

Principle	Classification	Detection Time	NDZ
Harmonics/THD	Passive (Grid voltage sensorless control) [32]	45 ms	None
Changes of impedance	Active (injecting a high frequency signal) [33]	A few ms	None
Power changes	Active (reactive power variation) [31]	Less than 2 s	None
Wavelet	Passive (wavelet packet transform) [34]	40 ms	Almost zero
Combination	Passive scheme (Fast Gauss Newton algorithm) [35]	Less than 20 ms	Very small
Proposed Method	Fast Discrete S-Transform and Cumulative Impedance Index	About 10 ms	Very small

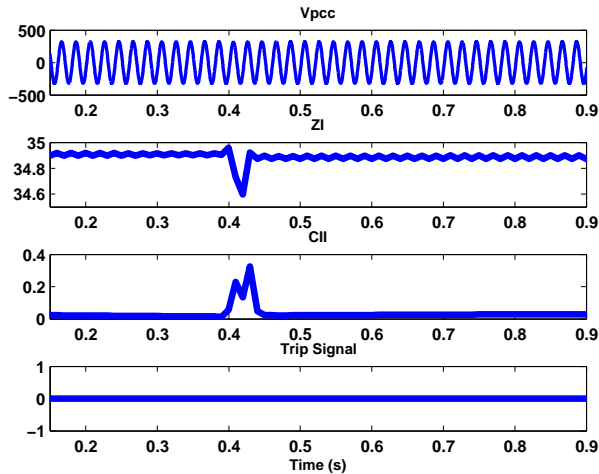


Fig. 16: System response for Case 5.

islanding is significant so that reliable threshold value could be selected. In order to have smaller NDZ and FDZ (Failing Detection Zone) threshold must be adjusted as Eq. (14):

$$\begin{aligned} \text{Max } CII \text{ of Normal Operation} &< \text{Threshold} \\ &< \text{Min } CII \text{ of Islanding Operation.} \end{aligned} \quad (14)$$

The worst cases of normal and islanding operations are Case 1 and Case 3. Therefore, multiple simulations with quality factors from 0.5 to 70 have been done for these cases. Results are shown in Fig. 17 and Fig. 18. According to the figures, threshold can easily be set at 2.5, and still, it ensures that there would not be nuisance trip or missed islanding.

In one recent study, [14], NDZ has been calculated for a combined UFP/OFP and frequency dependent impedance method, when NDZ was dependent on selected harmonics for reference threshold, but NDZ of the proposed method does not have this kind of dependency. So, combination of this method with UFP/OFP method and determining appropriate threshold value, as discussed above, could decrease the NDZ significantly and increase the reliability of detection, but as can be seen from Fig. 18, loads with very high-quality factors could put this method in NDZ. Table 1 compares detection time and NDZ of some detection methods, as can be seen, the proposed method has good results.

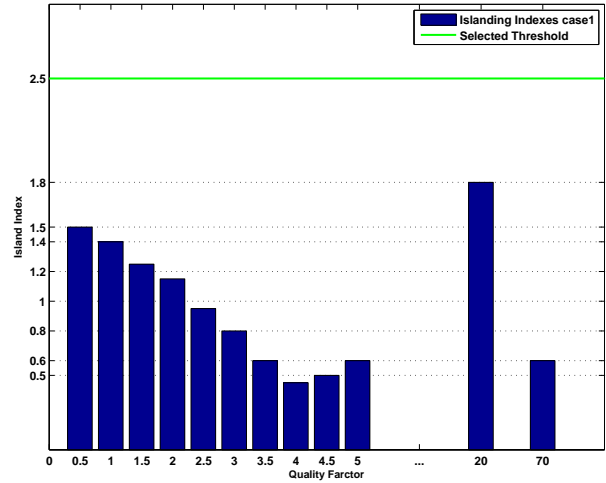


Fig. 17: CII of various Q_{fs} and selected threshold, Case 1.

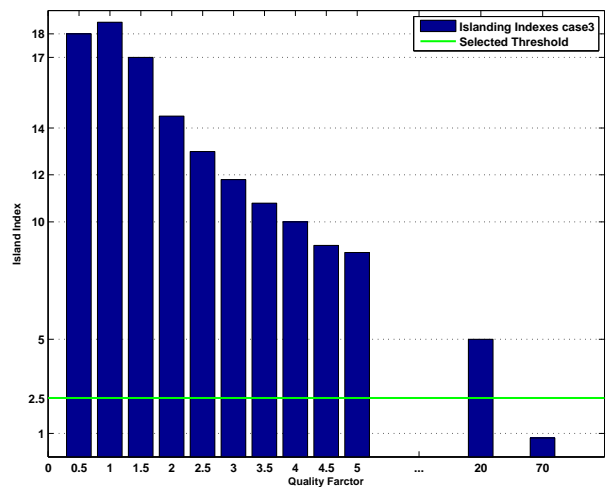


Fig. 18: CII of various Q_{fs} and selected threshold Case 3.

6. Conclusion

This paper proposed a new passive approach for islanding detection using summation of impedance of all frequencies seen at PCC. By measuring the voltage and current at the PCC and getting the S-transform of them, frequency dependent impedance is calculated. In this method, impedance is calculated for almost all frequencies rather than fundamental frequency alone. When islanding occurs, the frequency dependent impedance which can be seen by DG changes and

this change is the base of detection, here. Tracking the changes in cumulative impedance of frequencies detects islanding occurrence. As FDST is a time-frequency analysis technique, it gives almost exact information of islanding time. So, it reduces the detection time by selecting small sample time. The proposed method is not so sensitive to Non-linear loads, inductive loads and changes in load of grid. In addition, the proposed method decreases the NDZ, and it is reliable in presence of noise. Combining the proposed technique with some artificial intelligence methods or even using other modern analyzing methods like Variational Mode Decomposition (VMD) instead of S-Transform might help to get better results.

References

- [1] ALJANKAWAY, A. S., W. G. MORSE, L. CHANG and C. P. DIDUCH. Passive method-based islanding detection of Renewable-based Distributed Generation: The issues. In: *Electrical Power & Energy Conference*. Halifax: IEEE, 2010, pp. 1–8. ISBN 978-1-4244-8186-6. DOI: 10.1109/EPEC.2010.5697253.
- [2] LIDULA, N. W. A. and A. D. RAJAPAKSE. Microgrids research: A review of experimental microgrids and test systems. *Renewable and Sustainable Energy Reviews*. 2011, vol. 15, iss. 1, pp. 186–202. ISSN 1364-0321. DOI: 10.1016/j.rser.2010.09.041.
- [3] MAHAT, P., Z. CHEN and B. BAK-JENSEN. Review of islanding detection methods for distributed generation. In: *Third International Conference on Electric Utility Deregulation and Restructuring and Power Technologies*. Nanjing: IEEE, 2008, pp. 2743–2748. ISBN 978-7-900714-13-8. DOI: 10.1109/DRPT.2008.4523877.
- [4] MAHAT, P., Z. CHEN and B. BAK-JENSEN. Review on islanding operation of distribution system with distributed generation. In: *Power and Energy Society General Meeting*. San Diego: IEEE, 2011, pp. 1–8. ISBN 978-1-4577-1000-1. DOI: 10.1109/PES.2011.6039299.
- [5] KUNTE, R. S. and W. GAO. Comparison and review of islanding detection techniques for distributed energy resources. In: *40th North American Power Symposium*. Calgary: IEEE, 2008, pp. 1–8. ISBN 978-1-4244-4283-6. DOI: 10.1109/NAPS.2008.5307381.
- [6] JANG, S. I. A new islanding detection algorithm for distributed generations interconnected with utility networks. In: *Eighth IEE International Conference on Developments in Power System Protection*. Amsterdam: IEEE, 2004, pp. 571–574. ISBN 0-86341-385-4. DOI: 10.1049/cp:20040188.
- [7] DE MANGO, F., M. LISERRE, A. D. AQUILA and A. PIGAZO. Overview of Anti-Islanding Algorithms for PV Systems. Part I: Passive Methods. In: *12th International Power Electronics and Motion Control Conference*. Portoroz: IEEE, 2006, pp. 1878–1883. ISBN 1-4244-0121-6. DOI: 10.1109/EPEPEMC.2006.4778679.
- [8] DE MANGO, F., M. LISERRE and A. D. AQUILA. Overview of Anti-Islanding Algorithms for PV Systems. Part II: Active Methods. In: *12th International Power Electronics and Motion Control Conference*. Portoroz: IEEE, 2006, pp. 1884–1889. ISBN 1-4244-0121-6. DOI: 10.1109/EPEPEMC.2006.4778680.
- [9] SINGAM, B. and L. Y. HUI. Assessing SMS and PJD Schemes of Anti-Islanding with Varying Quality Factor. In: *IEEE International Power and Energy Conference*. Putra Jaya: IEEE, 2006, pp. 196–201. ISBN 1-4244-0273-5. DOI: 10.1109/PECON.2006.346645.
- [10] VIEIRA, J. C. M., W. FREITAS, Z. HUANG, W. XU and A. MORELATO. Formulas for predicting the dynamic performance of ROCOF relays for embedded generation applications. *IEE Proceedings - Generation, Transmission and Distribution*. 2006, vol. 153, iss. 4, pp. 399–406. ISSN 1350-2360. DOI: 10.1049/ip-gtd:20045205.
- [11] DANANDEH, A., H. SEYEDI and E. BABAEI. Islanding Detection Using Combined Algorithm Based on Rate of Change of Reactive Power and Current THD Techniques. In: *Asia-Pacific Power and Energy Engineering Conference*. Shanghai: IEEE, 2012, pp. 1–4. ISBN 978-1-4577-0547-2. DOI: 10.1109/APPEEC.2012.6307465.
- [12] JANG, S. I. and K. H. KIM. An Islanding Detection Method for Distributed Generations Using Voltage Unbalance and Total Harmonic Distortion of Current. *IEEE Transactions on Power Delivery*. 2004, vol. 19, iss. 2, pp. 745–752. ISSN 0885-8977. DOI: 10.1109/TPWRD.2003.822964.
- [13] YIN, J., C. P. DIDUCH and L. CHANG. Islanding Detection Using Proportional Power Spectral Density. *IEEE Transactions on Power Delivery*. 2008, vol. 23, iss. 2, pp. 776–784. ISSN 0885-8977. DOI: 10.1109/TPWRD.2007.915907.
- [14] LIU, N., A. S. ALJANKAWAY, C. P. DIDUCH, L. CHANG, J. SU and M. MAO. A new impedance-based approach for passive islanding detection scheme. In: *4th IEEE International Symposium on Power Electronics*

- for *Distributed Generation Systems*. Rogers: IEEE, 2013, pp. 1–7. ISBN 978-1-4799-0692-5. DOI: 10.1109/PEDG.2013.6785646.
- [15] LIDULA, N. W. A. and A. D. RAJAPAKSE. A Pattern Recognition Approach for Detecting Power Islands Using Transient Signals—Part I: Design and Implementation. *IEEE Transactions on Power Delivery*. 2010, vol. 25, iss. 4, pp. 3070–3077. ISSN 0885-8977. DOI: 10.1109/TPWRD.2010.2053724.
- [16] SAMUI, A. and S. R. SAMANTARAY. Wavelet Singular Entropy-Based Islanding Detection in Distributed Generation. *IEEE Transactions on Power Delivery*. 2013, vol. 28, iss. 1, pp. 411–418. ISSN 0885-8977. DOI: 10.1109/TPWRD.2012.2220987.
- [17] ISAZADEH, G., A. KHODABAKHSHIAN and E. GHOLIPOUR. A new intelligent wide area controlled islanding detection method in interconnected power systems. *International Transactions on Electrical Energy Systems*. 2017, vol. 27, iss. 7, pp. 23–29. ISSN 2050-7038. DOI: 10.1002/etep.2329.
- [18] GUO, X., X. ZHANG, B. WANG, W. WU and J. M. GUERRERO. Asymmetrical Grid Fault Ride-Through Strategy of Three-Phase Grid-Connected Inverter Considering Network Impedance Impact in Low-Voltage Grid. *IEEE Transactions on Power Electronics*. 2014, vol. 29, iss. 3, pp. 1064–1068. ISSN 0885-8993. DOI: 10.1109/TPEL.2013.2278030.
- [19] STRASSER, T., F. ANDREN and J. KATHAN. A Review of Architectures and Concepts for Intelligence in Future Electric Energy Systems. *IEEE Transactions on Industrial Electronics*. 2015, vol. 62, iss. 4, pp. 2424–2438. ISSN 0278-0046. DOI: 10.1109/TIE.2014.2361486.
- [20] SUMNER, M., A. ABUSORRAH, D. THOMAS and P. ZANCHETTA. Real Time Parameter Estimation for Power Quality Control and Intelligent Protection of Grid-Connected Power Electronic Converters. *IEEE Transactions on Smart Grid*. 2014, vol. 5, iss. 4, pp. 1602–1607. ISSN 1949-3053. DOI: 10.1109/TSG.2014.2298495.
- [21] CIOBOTARU, M., R. TEODORESCU, P. RODRIGUEZ, A. TIMBUS and F. BLAABJERG. Online grid impedance estimation for single-phase grid-connected systems using PQ variations. In: *IEEE Power Electronics Specialists Conference*. Orlando: IEEE, 2007, pp. 2306–2312. ISBN 978-1-4244-0654-8. DOI: 10.1109/PESC.2007.4342370.
- [22] KAREGAR, H. K. and B. SOBHANI. Wavelet transform method for islanding detection of wind turbines. *Renewable Energy*. 2012, vol. 38, iss. 1, pp. 94–106. ISSN 0960-1481. DOI: 10.1016/j.renene.2011.07.002.
- [23] DAI, D., X. WANG, J. LONG, M. TIAN, G. ZHU and J. ZHANG. Feature extraction of GIS partial discharge signal based on S-transform and singular value decomposition. *IET Science, Measurement & Technology*. 2017, vol. 11, iss. 2, pp. 186–193. ISSN 1751-8822. DOI: 10.1049/iet-smt.2016.0255.
- [24] STOCKWELL, R. G., L. MANSINHA and R. P. LOWE. Localization of the complex spectrum: the S transform. *IEEE Transactions on Signal Processing*. 1996, vol. 44, iss. 4, pp. 998–1001. ISSN 1053587X. DOI: 10.1109/78.492555.
- [25] STOCKWELL, R. G. Why use the S-transform? *American Mathematical Society*. 2007, vol. 52, iss. 1, pp. 279–309. ISSN 1088-6834.
- [26] KRISHNANAND, R. K. and P. K. DASH. A New Real-Time Fast Discrete S-Transform for Cross-Differential Protection of Shunt-Compensated Power Systems. *IEEE Transactions on Power Delivery*. 2013, vol. 28, iss. 1, pp. 402–410. ISSN 0885-8977. DOI: 10.1109/TPWRD.2012.2221749.
- [27] NAIK, C. A. and P. KUNDU. Power quality disturbance classification employing S-transform and three-module artificial neural network. *International Transactions on Electrical Energy Systems*. 2014, vol. 24, iss. 9, pp. 1301–1322. ISSN 2050-7038. DOI: 10.1002/etep.1778.
- [28] ZEINELDIN, H. H. and J. L. KIRTLEY. Performance of the OVP/UVF and OFP/UFV Method With Voltage and Frequency Dependent Loads. *IEEE Transactions on Power Delivery*. 2009, vol. 24, iss. 2, pp. 772–778. ISSN 0885-8977. DOI: 10.1109/TPWRD.2008.2002959.
- [29] YE, Z., A. KOLWALKAR, Y. ZHANG, P. DU and R. WALLING. Evaluation of Anti-Islanding Schemes Based on Nondetection Zone Concept. *IEEE Transactions on Power Electronics*. 2004, vol. 19, iss. 5, pp. 1171–1176. ISSN 0885-8993. DOI: 10.1109/TPEL.2004.833436.
- [30] IEEE Recommended Practice for Utility Interface of Photovoltaic (PV) Systems. *IEEE Std 929-2000*. 2000. ISBN 0-7381-1934-2. DOI: 10.1109/IEEESTD.2000.91304.
- [31] AHMAD, K. K. N. E., J. SELVARAJ and N. A. RAHIM. A review of the islanding detection methods in grid-connected PV inverters. *Renewable and Sustainable Energy Reviews*. 2013, vol. 21, iss. 1, pp. 756–766. ISSN 1364-0321. DOI: 10.1016/j.rser.2013.01.018.

- [32] LISERRE, M., A. PIGAZO, A. DELL'AQUILA and V. M. MORENO. An Anti-Islanding Method for Single-Phase Inverters Based on a Grid Voltage Sensorless Control. *IEEE Transactions on Industrial Electronics*. 2006, vol. 53, iss. 5, pp. 1418–1426. ISSN 0278-0046. DOI: 10.1109/TIE.2006.882003.
- [33] REIGOSA, D., F. BRIZ, C. B. CHARRO, P. GARCIA and J. M. GUERRERO. Active Islanding Detection Using High-Frequency Signal Injection. *IEEE Transactions on Industry Applications*. 2012, vol. 48, iss. 5, pp. 1588–1597. ISSN 0093-9994. DOI: 10.1109/TIA.2012.2209190.
- [34] DO, H. T., X. ZHANG, N. V. NGUYEN, S. LI and T. T. CHU. Passive islanding detection method using Wavelet Packet Transform in Grid Connected Photovoltaic Systems. *IEEE Transactions on Power Electronics*. 2016, vol. 31, iss. 10, pp. 6955–6967. ISSN 0885-8993. DOI: 10.1109/TPEL.2015.2506464.
- [35] PADHEE, M., P. K. DASH, K. R. KRISHNANAND and P. K. ROUT. A Fast Gauss-Newton Algorithm for Islanding Detection in Distributed Generation. *IEEE Transactions on Smart Grid*. 2012, vol. 3, iss. 3, pp. 1181–1191. ISSN 1949-3053. DOI: 10.1109/TSG.2012.2199140.

About Authors

Solgun SALIMI was born in 1981; received the B.Sc. in electrical engineering from the Faculty of Electrical Engineering, k. N. Toosi University, Iran, in 2003; she received M.Sc. from Aliabad Katoul Branch of Islamic Azad University, Iran, in 2017. Her research interests are power system analysis, islanding detection algorithms.

Amangaldi KOOCHAKI was born in 1981; received the B.Sc. in electrical engineering from the Faculty of Electrical Engineering, University of Tehran, Iran, in 2003; he received M.Sc. and Ph.D. from Amirkabir University of Technology, Iran, in 2003 and 2010, respectively. Now he is assistant professor in Aliabad Katoul Branch of Islamic Azad University, Iran. His research interests are power system analysis and protection, relay coordination and renewable energies.

Amin HAJIZADEH was born in 1980; received the B.Sc. in electrical engineering from the Faculty of Electrical Engineering, Ferdowsi University, Mashhad, Iran, in 2002, he received M.Sc. and Ph.D. from Khajeh Nasir Toosi University, Iran, in 2005 and 2010, respectively. Now he is associate professor in Aalborg University, Denmark. His research interests are renewable energy and smart grids, distributed generation and microgrids.